Reactions of Phosphate Radicals with Monosubstituted Benzenes. A Mechanistic Investigation

by **Janina A. Rosso**, **Paula Caregnato**, **Verónica C. Mora**, **Mónica C. Gonzalez***, and **Daniel O. Mártire***

Instituto de Investigaciones Fisicoquímicas Teóricas y Aplicadas (INIFTA), Facultad de Ciencias Exactas, Universidad Nacional de La Plata, Casilla de Correo 16, Sucursal 4, (1900) La Plata, Argentina (fax: –54 221 425 4642; e-mail: gonzalez@inifta.unlp.edu.ar, dmartire@inifta.unlp.edu.ar)

Dedicated to Prof. Dr. *Silvia E. Braslavsky* on the occasion of her 60th birthday

The kinetics and reaction mechanism of phosphate radicals with substituted benzenes, PhX (X = OH, Me, H, Cl, MeO, and CHO), were studied by flash photolysis and continuous irradiation of aqueous solutions containing potassium peroxodiphosphate ($K_4[(PO_3)_2O_2]$). The rate constants for the reactions of phosphate radicals with the aromatic contaminants PhX were measured and the reaction intermediates and products detected. A correlation between the logarithm of the rate constant for every substrate with $H_2PO_4^{\bullet}$, $HPO_4^{\bullet -}$, and $PO_4^{\bullet 2-}$ and the logarithm of the dissociation constant K_a for H_3PO_4, $H_2PO_4^-$, and HPO_4^{2-} was found. A general mechanism is proposed (*Scheme 1*), which accounts for the experimental results.

1. Introduction. – Numerous constituents of natural and atmospheric waters contribute to the photochemical and/or thermal production of highly reactive species, such as $HO^{\bullet}$ and $SO_4^{\bullet -}$ radicals, which contribute to the self-cleansing of the ecosphere. Moreover, aqueous-phase procedures for waste-water treatment are frequently based on these radicals as initiators of the oxidation of organic substrates. $HO^{\bullet}$ and $SO_4^{\bullet -}$ are able to oxidize most inorganic anions to secondary, less-reactive radicals [1]. In particular, the reactions with phosphate ions present in the aqueous matrix of contaminated waters yield phosphate radicals that may have unexpected consequences in the overall oxidation [2].

In previous articles, we investigated the reactivity of phosphate radicals towards organic substrates [3–5]. The bimolecular rate constants obtained for the reactions of several aromatic substrates with the phosphate radicals $H_2PO_4^{\bullet}$, $HPO_4^{\bullet -}$, and $PO_4^{\bullet 2-}$ correlate with the electron-withdrawing ability of the substituent, as expected from the electrophilicity of these radicals [3][4]. The proposed mechanism [5] includes both electron transfer from the aromatics to the phosphate radicals and formation of an adduct between phosphate radicals and the aromatics, which may eliminate phosphate ions leading to hydroxycyclohexadienyl radicals or phosphite ions yielding phenoxyl radicals.

Following this research line in the present work, we measure the rate constants for the reactions of phosphate radicals with aromatic contaminants PhX (X = OH, Me, H, Cl, MeO, and CHO) and study in detail the reaction intermediates of these reactions. This information is of importance for evaluating the potential use of phosphate radicals as initiators for the destruction of pollutants in contaminated waters and for an in-depth analysis of the reaction mechanism involved.

For this purpose, we generate phosphate radicals by UV irradiation of peroxodiphosphate (= hexaoxo-μ-peroxodiphosphate(4–)) anions $P_2O_8^{4-}$. The three acid-base forms of these phosphate radicals in water are related by fast equilibria [1–5]. To study the reactions of each of these forms, experiments were performed under controlled pH conditions, *i.e.*, pH 4, 7, or 10, where $H_2PO_4^{\bullet}$, $HPO_4^{\bullet -}$, or $PO_4^{\bullet 2-}$, respectively, are the main radicals present

$$P_2O_8^{4-} \rightarrow 2PO_4^{\bullet 2-}$$

$$H_2PO_4^{\bullet} \underset{pK_a 5.7}{\overset{-H^+}{\rightleftharpoons}} HPO_4^{\bullet -} \underset{pK_a 8.9}{\overset{-H^+}{\rightleftharpoons}} PO_4^{\bullet 2-}$$

2. Results and Discussion. – 2.1. *Reaction Kinetics.* The reactions of the phosphate radicals $H_2PO_4^{\bullet}$, $HPO_4^{\bullet -}$, and $PO_4^{\bullet 2-}$ with substituted benzenes (*Eqn. 1*) are conveniently studied by flash-photolysis by following the phosphate radical decay rate as a function of added solute concentration.

$$\begin{pmatrix} H_2PO_4^{\bullet} \\ HPO_4^{\bullet -} \\ PO_4^{\bullet 2-} \end{pmatrix} + PhX \xrightarrow{k_1} Products \qquad (1)$$

Photolysis experiments on $K_4P_2O_8$ solutions at pH 4.0, 7.1, and 10.0 in the presence of low concentrations of substrate ($[PhX] < 2 \cdot 10^{-4}$ M) showed absorption traces at $\lambda >$ 400 nm, recorded immediately after the flash of light, that agree with the spectra of the phosphate radicals [3–5]. The experimental traces could be well fitted to $\Delta A = \Delta A_0 \exp(-k_{app} \cdot t) + C$ (*Fig. 1*, inset). The very small constant term C (lower than 3% of the maximum absorbance) is associated with the absorption of longer-lived species, mainly organic radicals, formed following phosphate radical depletion [3–5]. The calculated wavelength-independent constant k_{app} linearly increases with the substrate concentration (see *Fig. 1*). The slopes of the linear plots in *Fig. 1* yield the bimolecular rate constants k_1 [3–5]. *Table 1* shows the values of k_1 for the different substituted benzenes studied in this work and for those aromatics for which the rate constants with the three phosphate radicals are known. All the rate constants determined here fall in the reported correlation between log k_1 and the substituent *Hammett* parameter σ^+ [3–5], thus implying that the transition state of the reaction may have either significant polar character or important resonance interaction with the substituents.

A linear correlation between the logarithm of the rate constant k_1 for every substrate given in *Table 1* with $H_2PO_4^{\bullet}$, $HPO_4^{\bullet -}$, and $PO_4^{\bullet 2-}$ and the logarithm of the dissociation constant K_a for H_3PO_4, $H_2PO_4^-$, and HPO_4^{2-} was also found (*Fig. 2*). *Table 1* also includes the slopes a of the plots in *Fig. 2* for the aromatic compounds. The observed a values lie within the range 0.1–0.2, showing an average value of 0.15 with a standard deviation of 0.03. The intercepts b of the plots of log k_1 *vs.* log K_a (*Fig. 2*) strongly depend on the nature of the substrate. The plot of the intercepts b *vs.* the *Hammett* parameters σ^+ yields the straight line shown in the inset of *Fig. 2*.

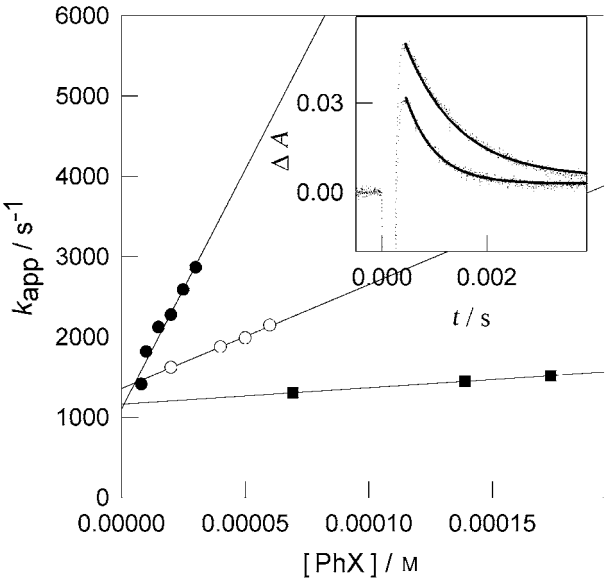

Fig. 1. *Plot of* k_{app} vs. [PhX] *for anisole* (●), *benzaldehyde* (○), *and chlorobenzene* (■) *obtained at pH 10*. Inset: *Absorbance profiles obtained at* $\lambda = 500$ *nm for* $8 \cdot 10^{-4}$ M $K_4P_2O_8$ *air-saturated solutions at pH 10 containing* $8 \cdot 10^{-6}$ M (upper trace) *and* $1.5 \cdot 10^{-5}$ M (lower trace) *anisole*. The solid lines show the first-order-fitting curves.

Table 1. *Bimolecular Rate Constants* k_1 [$M^{-1}s^{-1}$] *of the Reactions of the Phosphate Radicals* $H_2PO_4^{\bullet}$, $HPO_4^{\bullet-}$, *and* $PO_4^{\bullet 2-}$ *with Substituted Benzenes PhX, Substituent* σ^+_{min} *Values, and Slopes* a (see text)

PhX	k_1			σ^+_{min} [a])	a
	$H_2PO_4^{\bullet}$	$HPO_4^{\bullet-}$	$PO_4^{\bullet 2-}$		
Aniline	*ca.* 10^{10} [b])	$1.47 \cdot 10^9$ [b])	$7.1 \cdot 10^8$ [b])	1.30	0.108
Phenol	$(6.9 \pm 0.2) \cdot 10^8$ [c])	$(5.3 \pm 0.4) \cdot 10^8$ [d])	[e])	0.92	
Anisole	$(8.5 \pm 1.6) \cdot 10^9$ [c])	$(1.9 \pm 0.1) \cdot 10^8$ [f])	$(5.9 \pm 0.6) \cdot 10^7$ [c])	0.78	0.203
Benzyl alcohol	$(1.0 \pm 0.1) \cdot 10^9$ [g])	$(1.3 \pm 0.1) \cdot 10^8$ [g])	$(8.3 \pm 0.6) \cdot 10^7$ [g])		0.102
Toluene	$(5.2 \pm 0.5) \cdot 10^8$ [g])	$(1.4 \pm 0.1) \cdot 10^7$ [g])	$(1.4 \pm 0.1) \cdot 10^7$ [g])	0.31	0.147
Benzaldehyde	$(2.1 \pm 0.8) \cdot 10^8$ [c])	$(4.0 \pm 1.0) \cdot 10^7$ [c])	$(1.3 \pm 0.1) \cdot 10^7$ [c])		0.114
Benzene	$(8.9 \pm 0.5) \cdot 10^7$ [g])	$(1.7 \pm 0.2) \cdot 10^7$ [g])	$(4.3 \pm 0.3) \cdot 10^6$ [g])	0.00	0.124
Chlorobenzene	$(3.3 \pm 0.4) \cdot 10^7$ [c])	$(6.9 \pm 0.7) \cdot 10^6$ [d])	$(2.0 \pm 0.1) \cdot 10^6$ [c])	0.11	0.115
TFT [h])	$(3.5 \pm 0.5) \cdot 10^7$ [g])	$(2.7 \pm 0.5) \cdot 10^6$ [g])	$(9.0 \pm 1.0) \cdot 10^5$ [g])	0.57	0.149

[a]) From [6]. [b]) From [7]. [c]) This work. [d]) From [3]. [e]) At pH 10, phenolate is the main species. [f]) The value from [3] ($4.6 \cdot 10^7$ M^{-1} s^{-1}) was obtained from measurements of the decay rate constant of $HPO_4^{\bullet-}$ in the presence of solutions obtained by dilution of the anisole-saturated aqueous solution. The value reported here was corrected for the solubility of anisole at 25° determined in the present work ($2.28 \cdot 10^{-2}$ M). [g]) From [4]. [h]) α,α,α-Trifluorotoluene.

Phosphate radicals behave towards aromatics as oxidants. The efficiency of an oxidant does not necessarily depend solely on its redox potential. For instance, the hydroxyl radical, in spite of being a powerful one-electron oxidant, usually does not react by electron transfer but by addition [8]. This behavior is caused by the

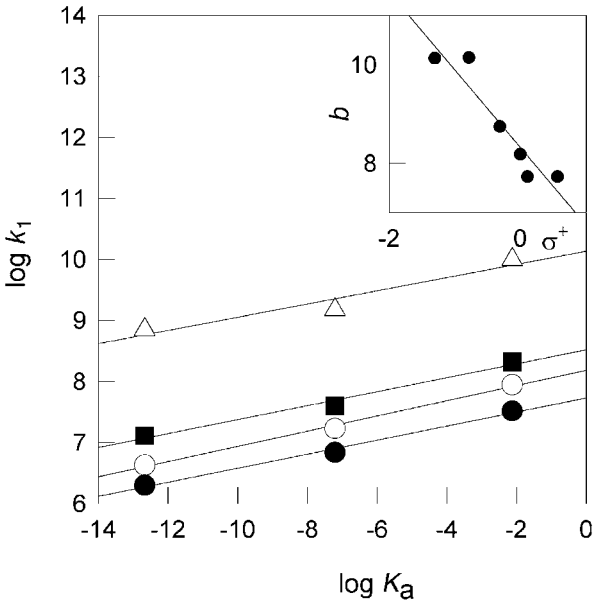

Fig. 2. *Plot of log* k_1 vs. *log* K_a *for aniline* (△), *benzaldehyde* (■), *benzene* (○), *and chlorobenzene* (●). Inset: *Plot of* b vs. σ^+.

stabilization of the transition state for addition by bond formation. The addition of OH• radicals to substituted benzenes PhX yields the hydroxycyclohexadienyl radicals (HOchdX•). To yield from this adduct the electron-transfer products (the radical cation and hydroxy anions), heterolysis of the C–OH bond must occur. However, since OH^- is a very poor leaving group, the rate of spontaneous heterolysis is very low. Thus, the reaction products are typically those obtained by dimerization or disproportionation of the HOchdX• radicals. One-electron oxidation products are observed only at low pH, where an acid catalysis may take place [9][10], *i.e.*, protonation of the OH group converts the poor leaving group OH^- (pK_a of its conjugate acid H_2O, 15.7) to the excellent leaving group H_2O (pK_a of its conjugate acid H_3O^+, -1.7) [8].

Sulfate radicals were proposed to react with aromatics by outer-sphere electron transfer [11], leading to electron-transfer products. However, *Steenken* [8], on the basis of a *Marcus* treatment and considering the redox potentials of the reactants, proposed that the electron-transfer products could be the result of an addition/elimination sequence, involving the formation of an adduct followed by sulfate ion elimination. Assuming *Steenken*'s mechanism, the different reactivity of hydroxyl and sulfate radicals lies in the leaving-group abilities of their redox partners, SO_4^{2-} and HO^- ions, respectively. The difference between the pK_a values of the conjugate acids, HSO_4^- (pK_a 1.9) and H_2O (pK_a 15.7) translates into a difference in the lifetimes of both adducts. In fact, the lifetime of the sulfate radical adduct with benzene was reported to be ≤ 100 ns [12][13], while the OH adduct (hydroxycyclohexadienyl radical) lives for milliseconds.

This behavior can be interpreted in terms of the *Brønsted* catalysis law (*Eqn. 2*), which expresses the relationship between the acidity constant K_a for an acid HA and its

catalytic constant k_{cat} for a given acid-catalyzed reaction [14]. The values of a for the reactions studied in the literature are found to be almost less than unity [14]. The plots shown in *Fig. 2* are *Brønsted* correlations (with $k_{cat} = k_1$ in *Eqn. 2*) that indicate that the observed rate constant k_1 depends on the leaving-group ability of each phosphate ion. This behavior can be rationalized assuming the formation of a σ adduct between the phosphate radicals and the aromatics and further elimination of phosphate ions. Therefore, the scheme proposed in [3] modifies to *Scheme 1* for $HPO_4^{\bullet -}$, where formation of the substrate radical cation **3** due to an addition/elimination route from substrate **1** *via* **2** is considered. Similar reactions can be written for the radicals $H_2PO_4^{\bullet}$ and $PO_4^{\bullet 2-}$, with elimination of $H_2PO_4^-$ and PO_4^{3-} ions, respectively, from the substrate–radical adduct corresponding to **2**.

$$\log k_{cat} = a \cdot \log K_a + b \tag{2}$$

Scheme 1

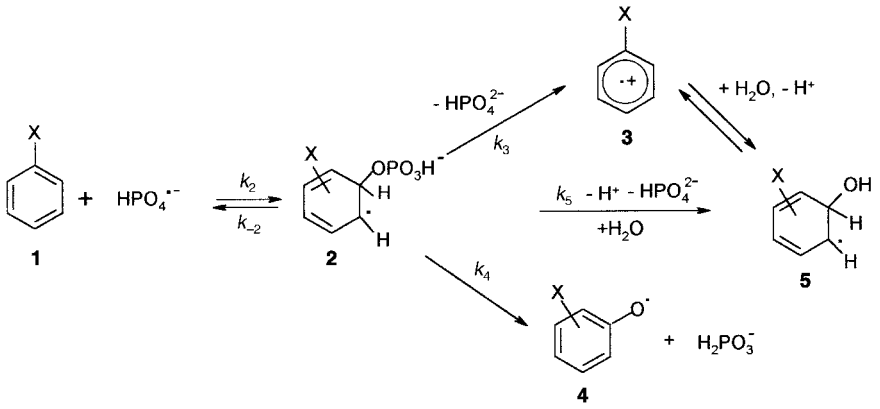

Since the phosphate ions are much better leaving groups than OH^-, a short lifetime is also expected for the σ adduct **2** or the corresponding adducts of $H_2PO_4^{\bullet}$ and $PO_4^{\bullet 2-}$ radicals, as for those of the sulfate radicals, in agreement with the lack of observation of these radicals in our experiments. This scheme considers phosphate (HPO_4^{2-}, $H_2PO_4^-$, or PO_4^{3-}) loss yielding the radical cation **3** of the aromatics as proposed for the sulfate adducts [8] and HOcdhX$^{\bullet}$ **5** as also suggested for the sulfate radical cation [15b]. Phosphite ($H_2PO_3^-$, H_3PO_3, or HPO_3^{2-}) elimination yielding phenoxyl radicals **4** was proposed in our previous investigations [3], in agreement with a similar pathway reported by *Merga et al.* [15b] for the sulfate radical.

A kinetics analysis of the mechanism proposed in *Scheme 1* assuming the steady-state condition for the phosphate radical adduct **2**, yields Eqn. 3 for k_1. This equation shows the proportionality between k_1 and k_2, as expected from the *Hammett* correlation found for different substrates (*vide supra*). However, k_1 is also affected by the decomposition rate of the σ adduct (through the rate constants k_{-2}, k_3, k_4, and k_5). Moreover, if $k_{-2} > (k_3 + k_4 + k_5)$, k_1 is also proportional to $k_3 + k_4 + k_5$, as expected from the observed *Brønsted* correlation, as for each radical $H_2PO_4^{\bullet}$, $HPO_4^{\bullet -}$, and

$PO_4^{\bullet 2-}$ both k_4 and k_5 depend on the elimination of $H_2PO_4^-$, HPO_4^{2-}, and PO_4^{3-}, respectively.

$$k_1 = k_2\left(\frac{k_3 + k_4 + k_5}{k_{-2} + k_3 + k_4 + k_5}\right) \quad (3)$$

The intercept b of the plots shown in *Fig. 2* can be interpreted as the value of $\log k_1$ for a much better leaving group ($K_a = 1$) than the three phosphate ions. The observed correlation between b and the *Hammett* parameters (*Fig. 2*, inset) further reflects the dependence of k_1 on k_2.

2.2. *Reaction Intermediates and Products.* Flash-photolysis experiments of peroxodiphosphate solutions in water containing almost saturated concentrations of the organic substrates show depletion of $H_2PO_4^{\bullet}$, $HPO_4^{\bullet -}$, and $PO_4^{\bullet 2-}$ radicals within less than 100 μs and the formation of transient species absorbing in the wavelength region 250–500 nm due to the organic radicals formed according to *Eqn. 1*. As the reactions of the radical $PO_4^{\bullet 2-}$ with the aromatics are not very efficient, the traces obtained from solutions at pH 10 show important absorbance contributions due to $PO_4^{\bullet 2-}$, thus hindering the identification of the organic radicals formed at this pH. Consequently, except for benzaldehyde, most of the absorption spectra of the organic radicals are not analyzed at pH 10. The observed intermediates and reaction products obtained for each substrate will be discussed separately. *Table 2* depicts the products observed in each case.

Table 2. *Observed Reaction Products of the Reaction of Dihydrogen and Hydrogen Phosphate Radicals with Substituted Benzenes in Aqueous Solution*

PhX	Phosphate radical	Products
Benzene	$H_2PO_4^{\bullet}$	phenol (15%)[a], CHOCH=CH–CO–CH_2OH, biphenyl[b])
Toluene	$H_2PO_4^{\bullet}$	benzaldehyde (11%), *p*-cresol
	$HPO_4^{\bullet -}$	benzaldehyde (4%), benzoate (41%)[c]), benzyl alcohol, bibenzyls
Phenol	$H_2PO_4^{\bullet}$	dihydroxybiphenyls[d])
Anisole	$H_2PO_4^{\bullet}$	2,2′-dimethoxybiphenyl
Chlorobenzene	$H_2PO_4^{\bullet}$	phenol (3%), 2-chlorophenol, 4-chlorophenol
Benzaldehyde	$HPO_4^{\bullet -}$	benzoate (100%)[c])

[a]) The percentages were calculated from a calibration curve with respect to the initial molar concentration of the substrate PhX. [b]) Detected only for conversions higher than 44%. [c]) Isolated as sodium salt. [d]) Distinction between the different isomers was not possible.

Benzene. The intermediates observed for the reactions of $H_2PO_4^{\bullet}$ and $HPO_4^{\bullet -}$ with benzene (**1**; X = H) show a very similar absorption around 310 nm, indicating that the same organic transient is formed for both phosphate radicals. The traces show a fast decay with a complex kinetics and formation of stable products. The transient spectrum obtained with N_2-saturated aqueous solutions is assigned to the hydroxycyclohexadienyl radical **5** (X = H) of benzene (OHchdH$^{\bullet}$, λ_{max} 315 nm). Radical **5** (X = H) reversibly reacts with molecular oxygen yielding peroxyl radical **6** (X = H) (*Scheme 2*). Lower concentrations of **5** and faster decay kinetics are observed in air- than in N_2-

saturated solutions. This behavior is rationalized by the existence of a reversible reaction between **5** and O_2, with $k_6 = 3.1 \cdot 10^8$ M^{-1} s^{-1} and $k_{-6} = 1.2 \cdot 10^4$ s^{-1} [16].

Scheme 2

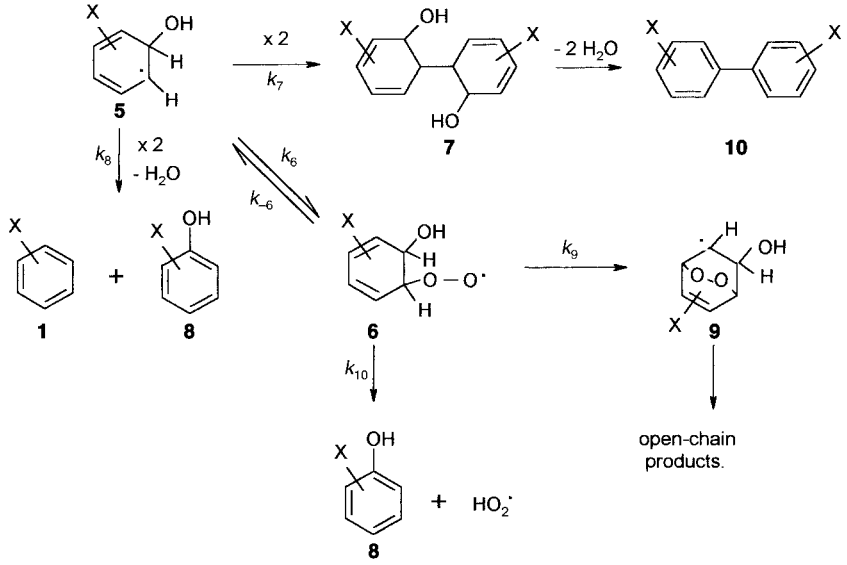

To support the presence of these reactions and neglect any possible contribution of the phosphate adduct to the observed spectrum, computer simulations of the traces obtained at 310 nm for the air-saturated solutions at pH 4 were done (see *Exper. Part* for details). The program considers a set of well established reactions involving reactions of phosphate radicals, **5** (X = H) and **6** (X = H): the reaction of *Eqn. 1* for the H_2PO_4· radical (see *Table 1* for k_1); the H_2PO_4· decay reactions in the absence of benzene [4]; the reactions **5** ⇌ **6** (k_6 and k_{-6}); the recombination reactions of **5** to **7** (k_7) and to **1**/**8** (k_8) (see *Scheme 2*), with $2(k_7 + k_8) = 7.3 \cdot 10^8$ M^{-1} s^{-1} [17], in agreement with the second-order kinetics observed for the decay of **5** in N_2-saturated solutions; recombination of **6**, with $2k_{REC} = 9 \cdot 10^8$ M^{-1} s^{-1} [2]; and reactions of **6** to **9** and to **8** with $k_9 + k_{10} = 800$ s^{-1} [16]. The simulated concentration profiles of **5** (X = H) and **6** (X = H) were converted into the corresponding absorbances taking $\varepsilon^{310} = 2270$ [17] and 300 M^{-1} cm^{-1} for **5** (X = H) and **6** (X = H), respectively. The ε^{310} value for **6** (X = H) was estimated from the spectrum reported in [18] and $\varepsilon^{300} = 500$ M^{-1}cm^{-1} taken from [16]. Since the radicals **5** (X = H) and **6** (X = H) are the main species contributing to the absorption traces at 310 nm, the addition of the absorbance contributions of **5** (X = H) and **6** (X = H) were compared with the experimental traces at this wavelength. A good agreement between experimental and simulated traces is found, as shown in the inset of *Fig. 3*, further supporting the assignment of the traces to the species **5** (X = H) and **6** (X = H).

Recombination of radicals **5** (X = H) leads to formation of biphenyl **10** (X = H) observed as a reaction product (see *Scheme 2*), or disproportionation of **5** (X = H) yields phenol (**8**; X = H; also detected) and benzene (**1**; X = H) with water elimination

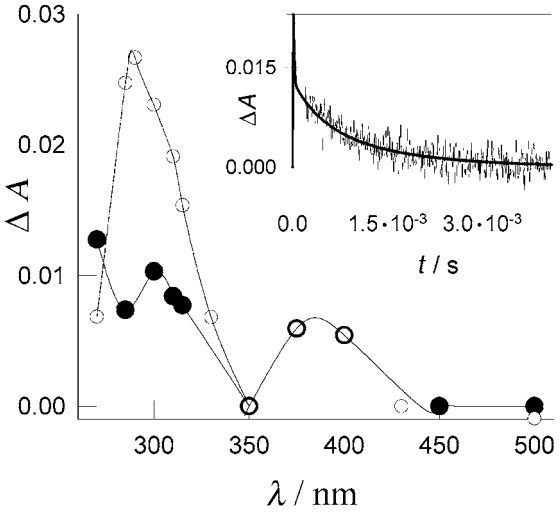

Fig. 3. *Transient absorption spectra obtained at 400 μs after the flash irradiation of 9.2 · 10⁻⁴ M $K_4P_2O_8$ solutions containing 5.6 · 10⁻⁵ M toluene at pH 4: air-saturated* (●) *and N_2-saturated* (○). Inset: *Experimental and simulated* (solid line) *absorbance profile obtained at 310 nm with 2.36 · 10⁻³ M $K_4P_2O_8$ air-saturated solution at pH 4 containing 4.8 · 10⁻³ M benzene.*

[19]. The peroxyl radical **6** (X = H) may rearrange to endoperoxide **9** (X = H) leading to the formation of open-chain oxidized products in agreement with the detection of CHOCH=CH–CO–CH_2OH (see *Scheme 2*). Otherwise, peroxyl radical **6** (X = H) eliminates $HO_2^{\bullet}$ yielding phenol (**8**; X = H).

Toluene: The intermediates of the reaction of $H_2PO_4^{\bullet}$ with toluene (**1**; X = Me) were analyzed in air- and N_2-saturated aqueous solutions. Both in the presence and absence of molecular oxygen, the absorption spectrum taken 400 μs after the flash of light shows an absorption band around 280–300 nm and a less-intense one in the 370–430 nm region, as shown in *Fig. 3*. The traces in the 280–300 nm region decay faster and are of lower amplitude in the presence of O_2. The traces in the 370–430 nm region show a second-order decay with $2k/\varepsilon^{400} = (3.2 \pm 1.5) \cdot 10^6$ cm s^{-1}, independently of the presence of O_2.

According to *Scheme 1*, the HOchdMe$^{\bullet}$ radical **5** (X = Me) and the phenoxyl radical **4** (X = Me) of toluene could be formed. Phenoxyl radicals exhibit an absorption maximum at *ca.* 300 nm and a less-intense one at around 400 nm, decay by second-order kinetics, and do not react with molecular oxygen [15]. The HOchdMe$^{\bullet}$ radical **5** (X = Me) shows an absorption maximum at 315 nm and reversibly reacts with molecular oxygen, yielding peroxyl radical **6** (X = Me), as already discussed for the HOchdH$^{\bullet}$ radical [16]. The absorption band in the 370–430 nm range is assigned to the phenoxyl radical **4** (X = Me) of toluene. Moreover, taking $\varepsilon^{400} \approx 1600$ M^{-1} cm^{-1} as for other phenoxyl radicals, we obtain $2k = 5.1 \cdot 10^9$ M^{-1} s^{-1}, which is of the same order as the value reported for the unsubstituted phenoxyl radical **4** (X = H; $2.3 \cdot 10^9$ M^{-1} s^{-1} [21]).

The benzyl radical **11** absorbing in the 250–290 nm range [20] can be formed by dehydration of **5** (X = Me) or by H^+ loss from the radical cation **3** (X = Me) [9] and reacts with molecular oxygen with a rate constant $k = 2.8 \cdot 10^9$ M^{-1} s^{-1} leading to the peroxyl radicals **12** (*Scheme 3*). Since the rate constants for the reactions of the three phosphate radicals with toluene fall in the corresponding *Hammett* correlations and, for this substrate, the straight line of the *Brønsted* correlation has a slope similar to those for the other PhX, formation of the benzyl radical **11** through H$^\cdot$ abstraction from the methyl group of toluene must not be a relevant reaction pathway.

Scheme 3

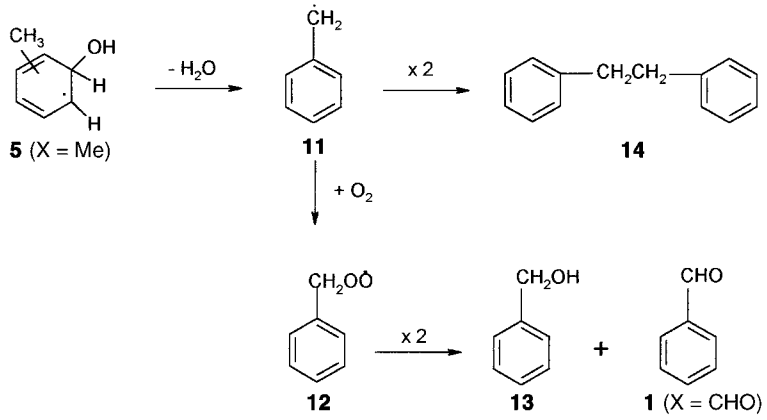

The ratio of the initial absorbances observed at 300 and 400 nm in N_2-saturated solutions, $\Delta A_o^{300}/\Delta A_o^{400}$, is higher than that expected for the phenoxyl raxical **4** (X = Me) [15], thus indicating that other radicals, such as **5** (X = Me) and benzyl radical **11**, contribute to the 280–330 nm absorption band. In fact, formation of benzaldehyde and *p*-cresol (=4-methylphenol) as reaction products support the participation of these radicals. Benzaldehyde (**1**; X = CHO) can arise from peroxyl radical **12** generated by reaction of the benzyl radical **11** with molecular oxygen (see *Scheme 3*). Formation of *p*-cresol (**8**; X = Me) is explained by disproportionation of **5** (X = Me) to **1**/**8** (X = Me), as shown in *Scheme 2*.

A similar absorption spectrum was obtained for the reaction of $HPO_4^{\cdot -}$ with toluene. The reaction products benzyl alcohol (**13**), benzaldehyde (**1**; X = CHO), benzoic acid, and bibenzyl **14** are all formed either by the oxidation of the benzyl radical **11** or from its recombination (*Scheme 3*).

Phenol. The intermediate formed by the reaction between $HPO_4^{\cdot -}$ and phenol (**1**; X = OH) with λ_{max} at 300 and 400 nm and a second-order-decay rate constant $2k = 1.7 \cdot 10^9$ M^{-1} s^{-1} was assigned to the phenoxyl radical **4** (X = H) [3][22]. A similar spectrum was found for the intermediate of the reaction of $H_2PO_4^\cdot$ with phenol in air-saturated solutions. This unsubstituted phenoxyl radical **4** (X = H) may be formed either by dihydrogen phosphate elimination from the σ adduct **2** (X = OH), as shown in *Scheme 4* for the $HPO_4^{\cdot -}$ reaction, or by the fast phosphate-catalyzed dehydration of the dihydroxycyclohexadienyl radical **5** (HOchdOH$^\cdot$) [23]. Formation of the dihy-

droxybiphenyl **10** (X = OH) observed as products for the reactions of $H_2PO_4^{\bullet}$ with phenol can be explained by C,C coupling of the unsubstituted phenoxyl radical **4** (X = H) and tautomerization (see *Scheme 4*) [24].

Scheme 4

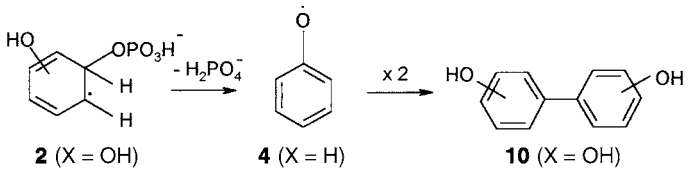

The hydroxyphenoxyl radical **4** (X = OH) with λ_{max} around 320 and 420 nm [25], which could be formed from the σ adduct **2** according to *Scheme 1*, is not observed, in agreement with the lack of detection of quinone and hydroquinone, formed after hydroxyphenoxyl radical disproportionation [21].

Anisole: The intermediates formed by the reaction of $H_2PO_4^{\bullet}$ and $HPO_4^{\bullet-}$ with anisole (**1**; X = MeO), 400 μs after the flash of light, show two absorption bands at 280–290 nm and 360–450 nm and a shoulder at 320 nm, shown in *Fig. 4* for the radical obtained from $HPO_4^{\bullet-}$. Due to the electron-donating character of the MeO group, stabilization of the radical cation **3** (X = MeO) of anisole is expected. The radical cation **3** (X = MeO) shows two absorption bands with maxima at 280 nm (ε^{280} = 7400 M^{-1} cm^{-1}) and at 430 nm (ε^{430} = 3200 M^{-1} cm^{-1}) [9]. The traces taken at 280 nm

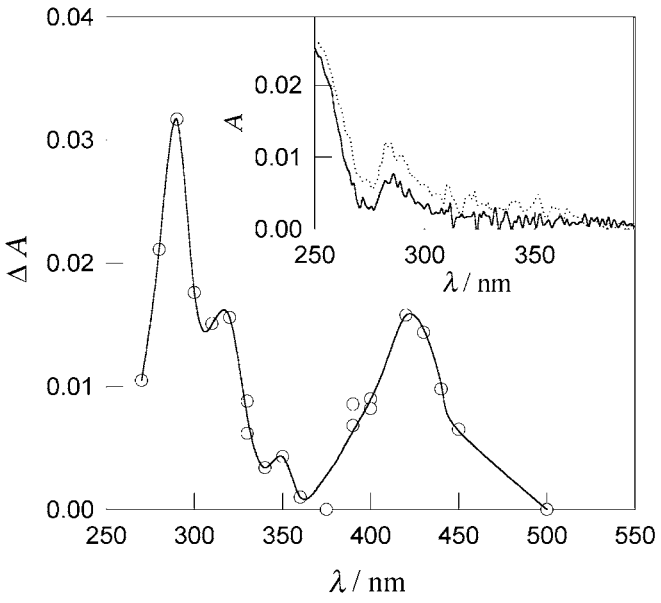

Fig. 4. *Transient absorption spectrum obtained at 400 μs after the flash irradiation of air-saturated 9.2 · 10⁻⁴* M *$K_4P_2O_8$ solutions containing 1.8 · 10⁻⁵* M *anisole at pH 7.* Inset: *Corresponding absortion spectra of the products at pH 4* (—) *and pH 7* (- - - -).

and in the 360–450 nm region follow a second-order decay both at pH 4 and 7. Taking the reported values of ε^{280} and ε^{430} for the radical cation **3** (X = MeO) [9], $2k = (2.5 \pm 0.8) \cdot 10^9$ M^{-1} s^{-1} is estimated in line with the value reported in [9] ($2k = 4 \cdot 10^9$ M^{-1} s^{-1}).

The traces at 320 nm show different decay kinetics, thus supporting the formation of a second intermediate. Formation of the HOchdOMe$^{\bullet}$ radical **5** (X = MeO) also absorbing at this wavelength ($\lambda_{max} = 320$ nm and $\varepsilon^{320} = 3400$ M^{-1} cm^{-1} [9]) must not be neglected. In acid medium, the HOchdOMe$^{\bullet}$ radical **5** (X = MeO) reversibly dehydrates, yielding the radical cation **3** (see *Scheme 1*) and, consequently, a higher contribution of this radical is expected at lower pH [26]. In fact, the traces obtained at pH 4 show higher initial absorbances than those at pH 7. The absorption spectra of the products formed at pH 4 and 7 are coincident (inset of *Fig. 4*). This spectrum corresponds to 2,2′-dimethoxybiphenyl, which was detected at pH 4 by GC/MS. Formation of dimethoxybiphenyls **10** (X = MeO) was reported to be due to recombination of the radical cation **3** (X = MeO) [9].

Chlorobenzene. The reaction of $HPO_4^{\bullet -}$ with chlorobenzene (**1**; X = Cl) leads to formation of phenoxyl radical **4** (X = Cl) [3] showing two absorption bands around 290–300 nm and in the 390–400 nm region, as shown in *Fig. 5*. Formation of the phenoxyl radical **4** (X = Cl) means that the reaction **2** → **4** in *Scheme 1* is an important reaction route for this substrate.

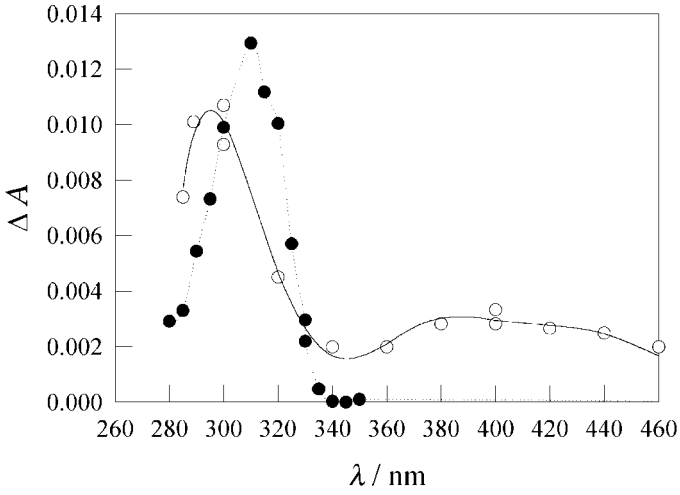

Fig. 5. *Transient absorption spectra obtained at 400 μs after the flash irradiation of air-saturated 9.2 · 10^{-4}* M *$K_4P_2O_8$ solutions containing 8.9 · 10^{-4}* M *chlorobenzene at pH 4* (●) *and 1.7 · 10^{-3}* M *chlorobenzene at pH 7* (○) [3]

The reaction of $H_2PO_4^{\bullet}$ with chlorobenzene shows an intermediate with absorption maximum at 315 nm (also shown in *Fig. 5*) whose decay kinetics and spectrum in air-saturated aqueous solutions are coincident with those reported [3] for the HOchdCl$^{\bullet}$ radical **5** (X = Cl) under identical experimental conditions and supported by formation of phenol and 2- and 4-chlorophenol as reaction products. Disproportionation of radical **5** (X = Cl) with loss of water yields chlorophenol **8** (X = Cl) and chlorobenzene (**1**; X = Cl) (for the *o*-, *m*-, and *p*-chloro-substituted radicals **5**, see *Scheme 2*). Loss of

HCl from the *ipso*-chloro-substituted isomer **5** yields phenol (**8**; X = H), as shown in *Scheme 5* [27]. The absence of the band at 400 nm indicates that formation of the phenoxyl radical **4** (X = Cl) is of no importance at this pH.

Scheme 5

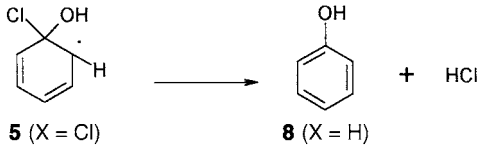

5 (X = Cl) **8** (X = H)

Benzaldehyde. The transient absorption spectrum obtained for the reaction of $H_2PO_4^{\bullet}$ with benzaldehyde (**1**; X = CHO) in the absence of molecular oxygen in aqueous solution, shows absorption maxima around 370 and 425 nm (*Fig. 6*) in agreement with that reported for the α,α-dihydroxybenzyl radical **15** ('hydrated' benzoyl radical) [19b][28]. Moreover, from a second-order-decay kinetic analysis and the ε value reported for the hydrated benzoyl radical **15**, $2k = (1.2 \pm 0.1) \cdot 10^9$ M^{-1} s^{-1} is obtained, in line with [29] ($> 8 \cdot 10^8$ M^{-1} s^{-1}). Any contribution of the naked benzoyl radical to the observed spectrum is of no significance because it shows a different absorption spectrum with a very low ε value ($\varepsilon = 150$ M^{-1} cm^{-1} at 370 nm [30]).

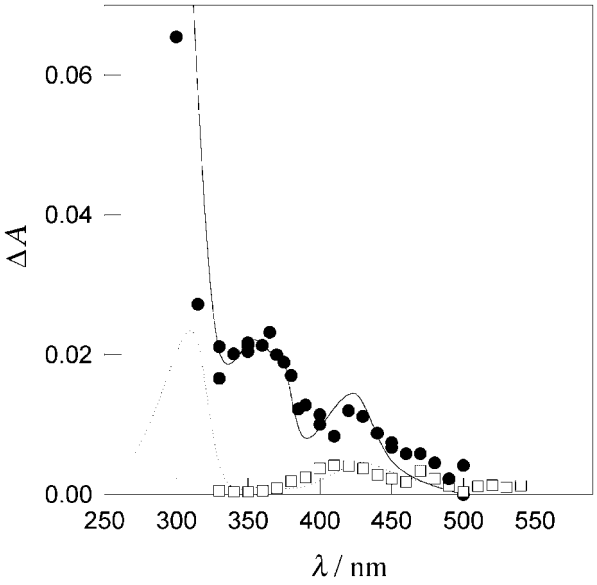

Fig. 6. *Transient absorption spectra obtained at 400 μs after the flash irradiation of Ar-saturated 9.2 · 10^{-4}* M *$P_2O_8^{-4}$ solutions containing 2.5 · 10^{-5}* M *benzaldehyde at pH 4* (●) *and 3.8 · 10^{-4}* M *$P_2O_8^{-4}$ solutions containing 3.1 · 10^{-5}* M *benzaldehyde at pH 7* (○). Published absorption spectrum of the benzoyl radical (solid line) and benzoyl radical anion (dotted line) [28].

In aqueous solutions aldehydes easily yield a 1,1-diol (benzaldehyde hydrate), which is more easily oxidized than the parent aldehyde. Since $H_2PO_4^{\bullet}$ reacts with aliphatic alcohols mainly by H-abstraction [29], $H_2PO_4^{\bullet}$ could abstract a H atom from

the hydrated form of benzaldehyde (which has a C–H bond dissociation energy of 88 kcal/mol) yielding an α,α-dihydroxybenzyl radical **15** [31] in equilibrium with its basic form, the corresponding radical anion **16**, as shown in *Scheme 6*. However, since the rate constants for the reactions of benzaldehyde with the three phosphate radicals fall in the correlation shown in *Eqn. 2* with a slope similar to those found for the other substituted benzenes (*Fig. 2* and *Table 1*), the mechanism shown in *Scheme 1* is also expected for this substrate. Formation of the hydrated benzoyl radical **15** is very likely due to phosphate elimination from the 2-(phosphatoxy)cyclohexadienyl radical **2** (X = CHO) to yield a radical cation **3** (X = CHO; see *Scheme 1*), which further deprotonates, yielding the hydrated benzoyl radical **15**.

Scheme 6

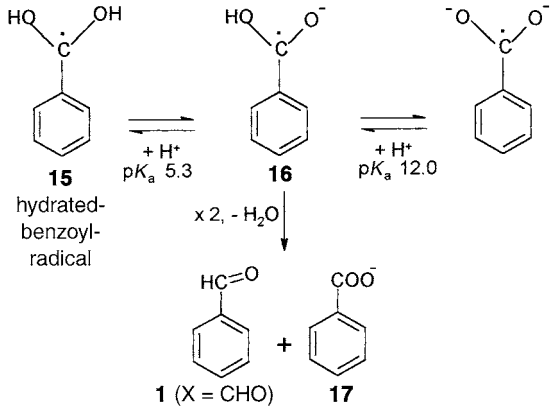

The transient of the reaction of $HPO_4^{\bullet -}$ and $PO_4^{\bullet 2-}$ with benzaldehyde in Ar-saturated solutions shows a broad absorption maximum around 430 nm coincident with that of the anion **16** of the α,α-dihydroxybenzyl radical [19b][28] obtained by deprotonation. From the second-order-decay kinetics and the reported ε values for the anion **16**, $2k = (1.4 \pm 0.5) \cdot 10^9$ M^{-1} s^{-1} and $(1.2 \pm 0.1) \cdot 10^9$ M^{-1} s^{-1} are obtained at pH 7 and 10, respectively. These values are higher than that reported ($7 \cdot 10^8$ M^{-1} s^{-1} [28]) at lower ionic strength, as expected from the ionic-strength effect on the recombination rate of two negatively charged ions.

Further disproportionation of the radical anion **16** leads to benzaldehyde (**1**; X = CHO) and benzoate (**17**); the latter, isolated as sodium salt, was the sole reaction product (*Scheme 6*).

3. Conclusions. – The presented results support *Scheme 1*. An addition pathway yields a phosphate-radical adduct **2** of the aromatic substrate. Such radical adducts are expected to be unstable (as is the case of the sulfate radical adducts [13], *vide supra*) and rapidly eliminate phosphate ions, yielding the radical cation **3** and the HOchdX$^{\bullet}$ radicals **5**, respectively. The radical cations **3** are stabilized in acid medium as observed for anisole (**1**; X = MeO). Otherwise, they decay to a more-stable radical, as may be the case of the formation of the 'hydrated' benzoyl radical **15** for the reaction with benzaldehyde (**1**; X = CHO). Radicals **5** can also be formed by reversible hydration of

the radical cations **3** [1][10] (*Scheme 1*). Evidence for the formation of the HOchdX$^{\bullet}$ radical **5** from the reactions of PhX with $H_2PO_4^{\bullet}$ and $HPO_4^{\bullet-}$ was found here for the substrates benzene (X = H), toluene (X = Me), chlorobenzene (X = Cl; only for the reaction with $H_2PO_4^{\bullet}$), and anisole (X = MeO). The formation of phenoxyl radicals **4** of toluene and chlorobenzene (only for the reaction with $HPO_4^{\bullet-}$) can be explained by phosphite loss from the phosphate adducts **2**.

The correlation shown in *Fig. 2* supports that the different k_1 values for $H_2PO_4^{\bullet}$, $HPO_4^{\bullet-}$, and $PO_4^{\bullet 2-}$ with every substrate could lie in the different leaving-group abilities of their redox partners, *i.e.*, $H_2PO_4^-$, HPO_4^{2-}, and PO_4^{3-}, respectively. This argument is further supported by the observation of the HOchdCl$^{\bullet}$ radical **5** (X = Cl) and the phenoxyl radical **4** (X = Cl) as intermediates for the reactions of chlorobenzene with the radicals $H_2PO_4^{\bullet}$ and $HPO_4^{\bullet-}$, respectively. Formation of **5** (X = Cl) in the reaction of $H_2PO_4^{\bullet}$ with chlorobenzene indicates the preferential loss of $H_2PO_4^-$, which is a better leaving group than HPO_4^{2-}.

Experimental Part

General. Tetrapotassium peroxodiphosphate (=tetrapotassium hexaoxo-μ-peroxodiphosphate(4−)) was electrochemically obtained as described in [4]. Chlorobenzene (*J. T. Baker*, p.a.), toluene (*Riedel-de-Haën*, p.a.), sodium benzoate (*Fluka*, p.a.), $CHCl_3$ (*Roth*, p.a.), benzene (*Merck*, p.a.), benzaldehyde (*Merck*, p.a.), phenol (*Fluka*, p.a.), anisole (*Fluka*, p.a.), KOH (*Riedel-de-Haën*, p.a.), $Na_2HPO_4 \cdot 2\ H_2O$ (*Merck*, p.a.), $NaH_2PO_4 \cdot H_2O$ (*Aldrich*, p.a.), and H_3PO_4 (*Merck*, p.a.) were used as received. Distilled water (>18 MΩ cm^{-1}, <20 ppb of org. C) was obtained from a *Millipore* system. The pH was adjusted with mixtures H_3PO_4/NaH_2PO_4, NaH_2PO_4/Na_2HPO_4, or K_2HPO_4/KOH to study the reactions of $H_2PO_4^{\bullet}$, $HPO_4^{\bullet-}$, or $PO_4^{\bullet 2-}$. The ionic strength of the solns. was within the range 0.1 – 0.2M.

Time-Resolved Experiments. Flash-photolysis experiments were carried out in a conventional apparatus (*Xenon Co.* model *720C*, 10 μs fwhm pulse) with modified optics and electronics [32]. The optical-path length was 20 cm. The emission of the flash lamps was filtered with sat. aq. solns. of the substrates in the water jacket of the cell to avoid photolysis of the aromatic compounds. The analysis source was a high-pressure mercury lamp (*Osram HBO-100 W*). To avoid product accumulation, each soln. was irradiated only once. When necessary, signals arising from single shots were averaged.

Steady-State Experiments and Product Analysis. Product analysis was performed in samples irradiated continuously. In the steady-state experiments, phosphate radicals were produced by UV photolysis of the peroxodiphosphate anion. A cylindrical low-pressure Hg lamp (*Heraeus*, *MNNI 35/20*, Germany) emitting at 254 nm was used. The photochemical reactor was of annular geometry (volume: 260 ml). The experimental conditions ($[P_2O_8^{4-}]_0 = 1$ m M and 0.2 m M ≤ $[PhX]_o$ ≤ 0.6 m M) were chosen to avoid possible PhX photolysis. Solns. of the aromatics were prepared by dilution of sat. aq. solns. at 25°.

Samples were taken at constant time intervals, and the total volume of sample withdrawn was always less than 5% the volume of the reactor. To avoid secondary reactions, products were analyzed at irradiation times lower than 6 min. Under these conditions, substrate consumption was kept below 15% in all cases. The reaction products formed after the reaction of phosphate radicals with the substituted benzenes were determined either by GC/MS or IC (ion chromatography).

For GC/MS analyses, org. substrates were extracted from the aq. solns. with a fixed volume of $CHCl_3$. The extracts were stored at 4° in glass vials with poly(tetrafluoroethene)/silicone septum-lined screw caps and minimized head space. GC/MS: *HP-6890* chromatograph equipped with a fused silica *HP5-MS GC* capillary column and coupled to an *HP 5973* mass-selective detector; temp. program from 30° to 320°; He as carrier gas, flow rate 29 ml s^{-1}; injection volume, 2 μl. Aliphatic compounds of low molecular mass, *i.e.*, containing four C-atoms or less, are eluted with the solvent in GC/MS determinations and could not be detected with our chromatographic set-up.

Anions evolution was performed by IC (*Dionex DX 500*) with suppressed conductivity detection: 4 × 250 mm *Ionpac AS11* (*Dionex*) column, 4 × 50 mm *Ionpac AG11* (*Dionex*) guard column, and 5 × 35 mm

(5 μm) *Ionpac NG1* (*Dionex*) guard column; eluent gradient program, flow rate, 1 ml min^{-1}; injection volume, 10 μl.

Kinetics Computer Simulations. A computer program based on the numerical resolution of the differential equations system by the third-order *Runge Kutta* method [32] was used to simulate the experimental absorbance profiles at 310 nm for experiments at pH 4 in the presence of 4.8×10^{-3} M benzene. The program considers the pulsed excitation as a delta function, producing $H_2PO_4^{\bullet}$ radicals. The concentration of $H_2PO_4^{\bullet}$ immediately after excitation, $[H_2PO_4^{\bullet}]_o = 1.3 \cdot 10^{-6}$ M, was taken as an input parameter, estimated from experiments under identical experimental conditions but in the absence of benzene.

This research was supported by the *Agencia Nacional de Promoción Científica y Tecnológica* (*ANPCyT*, Argentina). *J. A. R.* thanks the *Consejo Nacional de Investigaciones Científicas y Técnicas* (*CONICET*, Argentina), for a graduate studentship. *M. C. G.* is a research member of *CONICET*. *D. O. M.* is a research member of the *Comisión de Investigaciones Científicas de la Provincia de Buenos Aires* (*CIC*), Argentina.

REFERENCES

[1] A. B. Ross, W. G. Mallard, W. P. Helman, G. V. Buxton, R. E. Huie, P. Neta, 'NDRL-NIST Solution Kinetics Database: Ver. 3.0', Notre Dame Radiation Laboratory, Notre Dame, IN and National Institute of Standards and Technology, Gaithersburg, MD, 1998; http://www.rcdc.nd.edu.
[2] P. Maruthamuthu, P. Neta, *J. Phys. Chem*. **1978**, *82*, 710.
[3] S. S. Cencione, M. C. Gonzalez, D. O. Mártire, *J. Chem. Soc., Faraday Trans.* **1998**, *94*, 2933.
[4] J. A. Rosso, F. J. Rodríguez Nieto, M. C. Gonzalez, D. O. Mártire, *J. Photochem. Photobiol., A: Chemistry* **1998**, *116*, 21.
[5] D. O. Mártire, M. C. Gonzalez, *Prog. React. Kinet. Mechan.* **2001**, *26*, 201.
[6] J. March, in 'Advanced Organic Chemistry, Reactions, Mechanisms, and Structure', Wiley-Interscience, New York, 1991, p. 278.
[7] P. Subramanian, V. Ramakrishnan, J. Rajaram, J. C. Kuriacose, *Proc. Indian Acad. Sci. (Chem. Soc.)* **1986**, *97*, 573.
[8] S. Steenken, 'One Electron Redox Reactions between Radicals and Organic Molecules. An Addition/Elimination (Inner-Spere) Path', in *Top. Curr. Chem.*, Vol. 177, 'Electron Transfer II', Ed. J. Mattay, Springer, Berlin 1996, p. 125.
[9] J. Holcman, K. Sehested, *J. Phys. Chem.* **1976**, *80*, 1642.
[10] H. Mohan, J. P. Mittal, *J. Phys. Chem.* **1995**, *99*, 6519; H. Mohan, J. P. Mittal, *J. Phys. Chem. A,* **1999**, *103*, 379; H. Mohan, J. P. Mittal, *Chem. Phys. Lett.* **1995**, *235*, 444.
[11] P. Neta, V. Madhavan, H. Zemel, R. W. Fessenden, *J. Am. Chem. Soc.* **1977**, *99*, 163.
[12] S. Steenken, in 'Free Radicals in Synthesis and Biology', NATO ASI Series C – 260, Ed. F. Minisci, Kluwer Academic Publishers, Dordrecht, 1989, p. 220.
[13] S. Steenken, *J. Chem. Soc., Faraday Trans. 1* **1987**, *83*, 113.
[14] E. S. Gould, 'Mechanism and Structure in Organic Chemistry', Holt, Rinehart & Winston, New York, 1959, p. 113.
[15] a) J. Dzengel, J. Theurich, D. W. Bahnemann, *Environ. Sci. Technol*. **1999**, *33*, 294; b) G. Merga, C. T. Aravindakumar, B. S. M. Rao, H. Mohan, J. P. Mittal, *J. Chem. Soc., Faraday Trans.* **1994**, *90*, 597.
[16] C. von Sonntag, H.-P. Schuchmann, in 'The Chemistry of Free Radicals: Peroxyl Radicals in Aqueous Solutions', Ed. Z. B. Alfassi, John Wiley & Sons Ltd., Chichester, 1997, p. 173.
[17] G. V. Buxton, J. R. Langan, J. R. Lindsay Smith, *J. Phys. Chem.*, **1986**, *90*, 6309.
[18] L. M. Dorfman, I. A. Taub, R. E. Bühler, *J. Chem. Phys.* **1962**, *36*, 3051.
[19] a) M. K. Eberhardt, *J. Phys. Chem.* **1974**, *78*, 1795; b) J. A. Rosso, S. G. Bertolotti, A. M. Braun, D. O. Mártire, M. C. Gonzalez, *J. Phys. Org. Chem.* **2001**, *14*, 300.
[20] K. Sehested, H. Corfitzen, H. C. Christensen, E. J. Hart, *J. Phys. Chem.* **1975**, *79*, 310.
[21] G. N. R. Tripathy, R. H. Schuler, *Chem. Phys. Lett.* **1982**, *88*, 253.
[22] M. N. Schuchmann, E. Bothe, J. von Sonntag, C. von Sonntag, *J. Chem. Soc., Perkin Trans. 2*, **1998**, 791.
[23] E. J. Land, M. Ebert, *Trans. Faraday Soc.* **1967**, *63*, 1181.
[24] F. Berho, R. Lesclaux, *Chem. Phys. Lett.* **1997**, *279*, 289.
[25] E. J. Land, *J. Chem. Soc., Faraday Trans.* **1993**, *89*, 803.
[26] P. O'Neill, S. Steenken, K. Sehested, D. Schulte-Frohlinde, *J. Phys. Chem.***1975**, *79*, 2773 and ref. cit. therein.

[27] H. Mohan, M. Mudaliar, C. T. Aravindakumar, B. S. Madhav Rao, J. P. Mittal, *J. Chem. Soc., Perkin Trans. 2* **1991**, 1387.
[28] M. Simic, M. Z. Hoffman, *J. Phys. Chem.* **1972**, *76*, 1398.
[29] P. Maruthamuthu, P. Neta, *J. Phys. Chem.* **1977**, *81*, 1622.
[30] H. Fischer, R. Baer, R. Hany, I. Verhoolen, M. Walbiner, *J. Chem. Soc., Perkin Trans.2* **1990**, 787.
[31] K. B. Wiberg, F. Freeman, *J. Org. Chem.* **2000**, *65*, 573.
[32] M. L. Alegre, M. Geronés, J. A. Rosso, S. G. Bertolotti, A. M. Braun, D. O. Mártire, M. C. Gonzalez, *J. Phys. Chem. A* **2000**, *104*, 3117.

Received December 3, 2002